Proceedings World Geothermal Congress 2015
Melbourne, Australia, 19-25 April 2015

# Utilization of Chloride Bearing High Enthalpy Geothermal Fluid

Gudrun Saevarsdottir[1], Steindor Hjartarson, Kristinn Ingason[2], Bjarni Palsson[3], William Harvey[4]

[1]Reykjavik University, Menntavegur 1, 101 Reykjavik

gudrunsa@ru.is

[2]Mannvit Engineering, [3]Landsvirkjun, [4]Power Engineers

**Keywords:** supercritical power cycles; IDDP; wet scrubbing; dry scrubbing; utilization of geothermal fluid; HCl; volatile chloride; corrosion mitigation; superheated geothermal steam

## ABSTRACT

The superheated Chloride Bearing geothermal fluid form IDDP-1 poses special challenges to the design of the utilization equipment. Chloride in the steam forms a potent acid at the onset of condensation which causes severe and rapid corrosion unless it is removed beforehand. In this work the thermodynamic powerplant design is considered for a range of steam treatment options for removal of the harmful compounds. The goal is to determine the best option to utilize such a steam, with regard to exergy conservation and cost

## 1. INTRODUCTION

Corrosion is one of the main operational problems in geothermal power plants working with high enthalpy fluids. The cause and severity of the corrosion varies between boreholes. Hydrogen chloride is an especially hazardous compound that can cause severe pitting corrosion when it dissolves in water. If this happens in a turbine, cracks can form at the bottom of the pits, which will grow larger with corrosion fatigue and lead to a final breakdown. There are methods to remove the harmful substances, or deal with this problem in other ways, to prevent such damage. The work in this paper was carried out in relation to the superheated IDDP-1 well at Krafla in Iceland and the results have been published by Hjartarson et. al.

### 1.1 Wet Scrubbing

Wet scrubbing is a commonly used method to remove harmful substances from industrial flue gases, or other gas streams. The most widely used corrosion mitigation is called wet scrubbing (WS). This technique can be applied to neutralise the chloride in the gas, as it will dissolve and react with chemicals in the wet scrubbing fluid. The basic technique is to inject liquid water with dissolved NaOH (NaOH is used in this study, although other compounds are available with similar results) into a stream of superheated steam. The liquid cools the steam down to saturation, forming a liquid phase. After the HCl has dissolved in the liquid phase the following reaction takes place.

$$NaOH + HCl \rightarrow NaCl + H_2O$$

After the reaction, the flow enters a separator, parting the clean steam and the contaminated liquid. The injected water cools the steam down, resulting in a loss of superheat. The injection liquid that enters the system increases the total mass flow, and enthalpy is conserved in the process, but the loss of the superheat causes loss of exergy; which again leads to less recoverable energy.

### 1.2 Dry Steam Scrubbing

Another method which is under development and gaining attention is dry scrubbing (DS). DS does not require any cooling of the superheated steam. Solid or liquid material is either injected into the stream in a length of a pipe or in a reactor vessel built into the pipeline (Fisher et al., 1996). When the chemicals have mixed with the flow, it is driven through some sort of a separator, such as an electrostatic precipitator or a bag house filter, where the injected material is filtered out, along with the adsorbed or absorbed contaminants (Fisher et al., 1996). The waste material can often be cleaned and reinjected and thereby recycled to lower operational costs and reduce waste.

There are two similar ways to implement a solid-phase DS; absorption and adsorption. Absorption is a chemical reaction between then contaminates and the injected material (absorbent), while in the case of adsorption, the chemical attaches to the surface of the adsorbate without a direct chemical reaction. It is easier to recycle the adsorbent that the absorbent, which does not only lower operational costs but also, cost of disposal (Fisher et al., 1996).

Salt dissolved in water has strong electric fields that keep the solution in liquid phase at conditions where water would normally evaporate. The solubility of a salt is proportional to the strength of the electric field, that is, liquid salt solution can coexist with more superheated steam as the solubility of the salt increases.

Potassium carbonate ($K_2CO_3$) is a salt with high solubility and can therefore coexist with superheated steam to some degree (Weres et al. 2010). The reaction between $K_2CO_3$ and HCl is the following

$$K_2CO_3 + 2HCl \rightarrow 2KCl + CO_2 + H_2O$$

### 1.3 Binary Cycle

Binary cycle has also been introduced to the discussion in this context. The heat exchanger in the power cycle that condenses a superheated geothermal steam containing HCl may suffer severe corrosion. The corrosion hasn't been eliminated, it has rather been shifted from the turbine over to the heat exchanger.

Although this may not strictly categorize as corrosion mitigation, it is from the standpoint of the turbine and is worth looking into. The reason is that heat exchangers can tolerate the same rate of corrosion longer than turbines before break down for they have no moving parts causing corrosion fatigue to accelerate the process. There is also more room for material selection when constructing the instrument than in the case of turbines.

It has to be noted that when handling the dry boreholes from the IDDP it is hard, maybe even impossible, to keep the wellhead pressure of the geofluid such that it does not flash. The reason is that it seems that the steam in IDDP-1 is dry out to the fractures in the rock outside the borehole. For that reason, it is assumed that the heat exchanger will have superheated steam at the inlet and the corresponding condensate at the outlet.

This study will examine the utilization efficiency of each corrosion mitigation method, and determine if they pay off.

### 1.4 IDDP

The Icelandic Deep Drilling Project (IDDP) has the main goal of finding out if it is technically and economically feasible to extract supercritical fluids from hydrothermal systems. The intention is to access fluid at supercritical conditions and bring it to the surface as superheated steam (600 – 800°C) at subcritical pressure (< 220bar). One attempt has been made to drill such a borehole, which ended in a magma intrusion at 2104m depth, which is not sufficient to obtain supercritical pressures. The shallow depth entails downhole pressure of around 120bar, with enthalpy of around 3150kJ/kg. This borehole, IDDP-1, contains volatile chloride and other contaminants that require the geofluid to undergo special treatment before utilization.

### 1.5 Chloride induced corrosion

Geothermal steam containing volatile chloride is found in steam fields throughout the world, such as Krafla in Iceland, Laraderello in Italy, Saint Lucia in Windward Islands, Tatun in Taiwan, and The Geysers in USA (Hirtz et al. 1990). Most geothermal researchers agree that volatile chloride is transported as hydrogen chloride, HCl, although this has only been reported a few times (Hirtz et al. 1990)

When HCl comes in contact with liquid, the compound parts into hydrogen and chloride ions. HCl doesn't cause any considerable damage when the steam temperature is above dew point, but when it cools below the acid dew point and droplets start to form in the gathering equipment. The HCl readily dissolves in the droplets, forming strong hydrochloric acid, and rapid pitting corrosion can take place. Stress corrosion cracking can also happen in the turbine, where cracks form at the bottom of a pit and propagate by corrosion fatigue leading to a final mechanical break (Viviani et al., 1995). HCl is usually only threatening when small amounts of liquid are present, since its concentration can be very high which accelerates the process of corrosion, but if large amounts of liquid are present then the hydrochloric acid becomes more dilute and not necessarily of any particular concern.

It is the simultaneous attack of hydrogen and chloride ions that is especially damaging (Meeker et al., 1990). First, the chloride ion breaks the magnetite film on the steel surface, $Fe_3O_4$, which protects the metal against damage from many other chemicals. This is shown in the following chemical reaction.

$$Fe_3O_4 + 8HCl \rightarrow FeCl_2 + 2FeCl_3 + 4H_2O$$

After the breaking of the film, the hydrogen ion has direct access to the metal and the actual corrosion occurs by the following electrochemical reaction (Hirtz et al. 1991).

$$Fe^{+}[\![2H]\!]^{+} \rightarrow [\![Fe]\!]^{+2} + H_2$$

The chloride ion does not participate directly in the corrosion, it rather accelerates the process. This happens both by electrically balancing the rapid build-up of positively charged metal ions as well as enhancement by migration of the ions beneath scale deposits, where the ions can hydrolyze, generating HCl (Hirtz et al. 1991). This happens with the following chemical reaction, where the chlorine ions that initially parted from the hydrogen has reacted with iron(II), the product of reaction shown above.

$$FeCl_2 + 2H_2O \rightarrow Fe(OH)_2 + 2HCl$$

The breaking of the magnetite film inside the gathering equipment, the neutralization of the build-up of iron(II) (which, in other cases, hinders additional hydrogen ions to access the corrosion) and the production of more HCl is what makes the compound especially hazardous. It is therefore essential to both neutralize the acid and remove the chloride ions simultaneously (Meeker et al. 1990).

It should be noted that these chemical reactions may vary, depending on other chemicals present in the steam, such as oxygen, ammonia and boron for they may affect how the corrosion takes place.

An example of such corrosion is in Krafla, Iceland. A well produced 20 − 100ppmw chloride in superheated steam that resulted in corrosion rates of over 20mm/year. Excessive corrosion of 13% chromium steel turbine blade test coupons that were exposed to this steam was also observed (Hirtz et al. 1991).

## 2. METHOD

Six different software models for different equipment configurations were constructed, each with its own implementation of the corrosion mitigation methods mentioned above. All processes in the models are assumed to be adiabatic unless otherwise specified. Equipment and instruments in the power cycles are considered frictionless and horizontal; excluding kinetic and potential energy effects. And condensation in heat exchangers is assumed to be isobaric. These assumptions do not affect the credibility of the results for some of the presumptions, such as mass flow rate from IDDP-1, are not conclusive, for the borehole has not been studied at steady state. This study will give an order of magnitude for the performance of each mitigation method, and rank them internally, working with a geofluid similar to the one from IDDP-1.

### 2.1 Energy Conversion

2.1.1 Turbine Expansion

Expansion of steam inside a turbine is modeled as dry expansion for superheated steam or wet expansion for saturated steam, depending on the nature of the power cycle. The dry turbine isentropic efficiency is assumed to be constant at 85% and the Baumann rule is used in order to account for degradation in turbine performance due to moisture present in wet expansion (DiPippo, 2008). Wet turbine isentropic efficiency is given by

$$\eta_{tw} = \eta_{td} \ (1 + x_{outlet})/2 \tag{1}$$

The relation between the enthalpy of the geofluid and the isentropic turbine efficiency of the turbine is given by

$$\eta_t = (h_{in} - h_{out})/(h_{in} - h_{s,out}) \tag{2}$$

The following equation is used to determine the enthalpy of the fluid at the turbine outlet (DiPippo, 2008)

$$h_{out} = \frac{\left(h_{in} - 0.425(h_{in} - h_{out})\left(1 - h_{f,out}/(h_{g,out} - h_{f,out}\ )\right)\right)}{1 + \left(0.425(h_{in} - h_{s,out}\ )/(h_{g,out} - h_{f,out}\ )\right)} \tag{3}$$

When the fluid entering the turbine is superheated steam, the modeling of the expansion is split in two. The pressure where the steam crosses the saturation curve is found by trial-and-error.The specific power output of the turbine is given by

$$\eta_t = (h_{in} - h_{out})/(h_{in} - h_{s,out})\dot{W}_t/\dot{m} = h_{in} - h_{out} \tag{4}$$

2.1.2 Condenser

Condensing the liquid and vapor mixture to saturated liquid is carried out in the condenser. At steady state, mass and energy balances for a control volume enclosing the condensing side of the heat exchanger and a control volume enclosing the cooling medium side, respectively, give

$$\dot{Q}_{out}/\dot{m}_{gf} = h_{gf,in} - h_{gf,out} \tag{5}$$

$$\dot{Q}_{in}/\dot{m}_{cm} = h_{cm,out} - h_{cm,in} \tag{6}$$

Energy balance across the condenser gives

$$\dot{m}_{gf}(h_{gf,in} - h_{gf,out}) = \dot{m}_{cm}(h_{cm,out} - h_{cm,in}) \tag{7}$$

2.1.3 Cooling Tower

A wet cooling tower with an induced-draft counter flow is used to cool the medium (water) in the condenser. The waste heat is rejected to the atmosphere with cooling water recirculating and serving as a transport medium for the heat transfer between the source (geofluid) and the sink (atmosphere) (Cengel, et al. 2006).

Applying the first law of thermodynamics to the cooling tower, gives the following relations, assuming steady flow and overall adiabatic conditions, with reference to figure 1

$$\dot{m}_b h_b + \dot{m}_x h_x = \dot{m}_c h_c + \dot{m}_y h_y \tag{8}$$

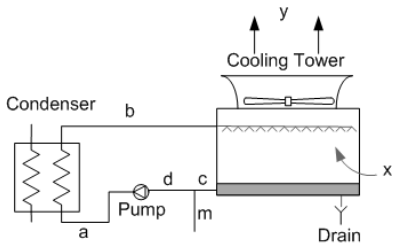


**Figure 1: Schematic diagram of a cooling tower.**

In order to account for evaporation of the cooling water and the corresponding water uptake of the air, the mass conservation of water and air are evaluated given, respectively, by

$$\dot{m}_b + \dot{m}_{wx} = \dot{m}_c + \dot{m}_{wy} \quad (9)$$

$$\dot{m}_{ax} = \dot{m}_{ay} \quad (10)$$

The surrounding air is assumed to be constant at 2.5°C, which was the average temperature at a weather station situated at Bjarnarflag, near IDDP-1, over the last 4 years.

2.1.4 Heat Exchanger in a Binary Cycle

The analysis of the heat exchanger in a binary cycle is a straightforward application of the principles of thermodynamics and mass conservation. The governing energy balance for the instrument, with reference to figure 7, is

$$\dot{m}_{gf}(h_1 - h_4) = \dot{m}_{wf}(h_b - h_e) \quad (11)$$

The heat exchanger is divided in three parts during modeling, to ensure that temperatures of the geofluid are greater than the ones of the working fluid at all stages; preheater, evaporator and superheater (named after the thermodynamical process that the working fluid is undergoing at each time). The temperatures of the geofluid between each stage are found using the known properties of the working fluid at all stages along with the two following energy balances across the preheater and evaporator, respectively

$$\dot{m}_{gf}(h_3 - h_4) = \dot{m}_{wf}(h_c - h_b) \quad (12)$$

$$\dot{m}_{gf}(h_2 - h_3) = \dot{m}_{wf}(h_d - h_c) \quad (13)$$

2.1.5 Feed Pump in a Binary Cycle

The specific work required to raise the pressure of the working fluid, with reference to figure 7, is given by

$$\dot{W}_p/\dot{m} = h_b - h_a \quad (14)$$

Using an isentropic efficiency of 80%, the enthalpy at state b is found with the following relation

$$\eta_p = (h_b - h_a)/(h_{s,b} - h_a) \quad (15)$$

2.1.6 Injection of Alkali Liquid in Wet Scrubbing

In order to apply wet scrubbing, the superheated steam has to be cooled down until its quality is 98% (Hirtz et al. 1990). The following energy balance for the node 1-2-7, with reference to figure 3, is used to determine how much water at T7 is required to be injected to get the desired quality at state 2

$$\dot{m}_1 h_1 = \dot{m}_2 h_2 + \dot{m}_7 h_7 \quad (16)$$

2.1.7 Utilization Efficiency

Using the second law of thermodynamics, the efficiency of the power cycle can be measured with respect to the maximum, theoretically attainable power output. The utilization efficiency is given by the following equation, where e is the specific exergy of the geofluid at the wellhead with respect to the surroundings

$$\eta_u = \dot{W}_{t,net}/(\dot{m}_{gf} e) \quad (17)$$

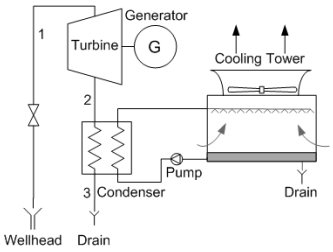


**Figure 2: Schematic diagram of a dry steam cycle**

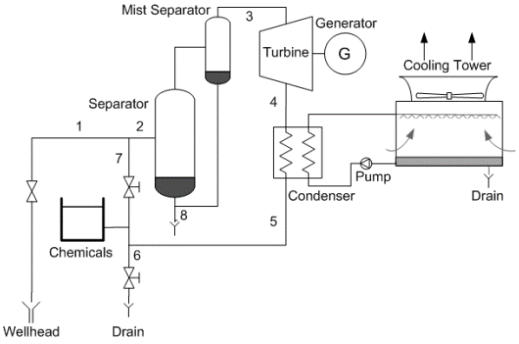


**Figure 3: Schematic diagram of a single-flash cycle with wet scrubbing**

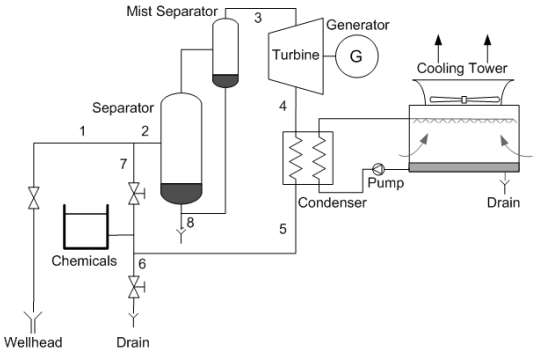


**Figure 4: Schematic diagram of a single-flash cycle with wet scrubbing and heat recovery**

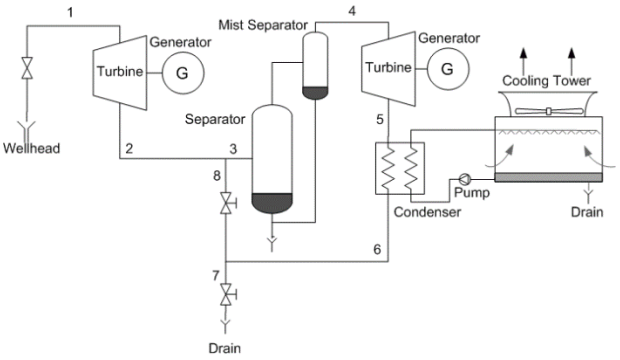


**Figure 5: Schematic diagram of a single-flash cycle with an additional turbine.Figure 2: Schematic diagram of a dry steam cycle**

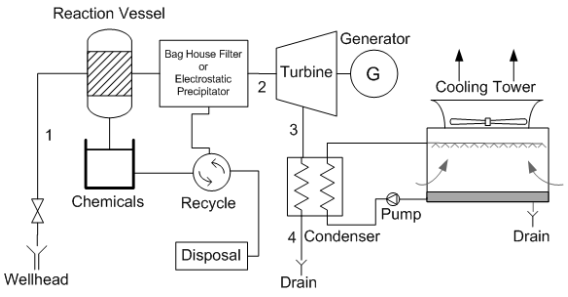


**Figure 6: Schematic diagram of a dry steam cycle with dry scrubbing**

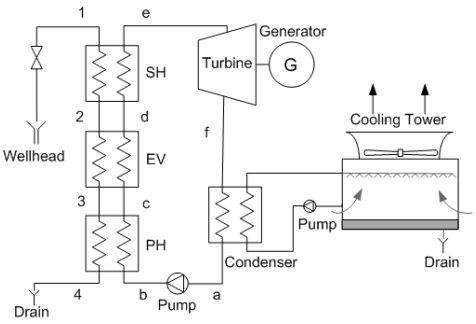


**Figure 7: Schematic diagram of a binary cycle**

### 2.2 Description of Individual Power Cycles

2.2.1 Dry Steam Cycle without Corrosion Mitigation

A process diagram of the power cycle is shown in figure 2. The superheated steam is led into a turbine where both dry and wet expansions takes place. After that the fluid enters the condenser where it cools down.

2.2.2 Single-Flash Cycle with Wet Scrubbing

A process diagram is shown in figure 3. Before the superheated geofluid enters the separator, enough liquid water is injected into the steam to cool it down to a point where its quality is 98%, according to equation x As said above, the injected water contains dissolved NaOH to fight corrosion. Since the fluid at state 3 contains no significant superheat, the turbine expansion is assumed to be solely wet. Next, the fluid enters the condenser and cools down.

2.2.3 Single-Flash Cycle with Wet Scrubbing and Heat Recovery.

A process diagram is shown in figure 4. Before the superheated geothermal steam undergoes traditional wet scrubbing, it enters a heat exchanger where it cools down. At the outlet of the heat exchanger, the fluid has 20°C of superheat, which should be enough to ensure that no condensation takes place. Next, enough liquid water is injected into the steam to cool it down. When the stream has

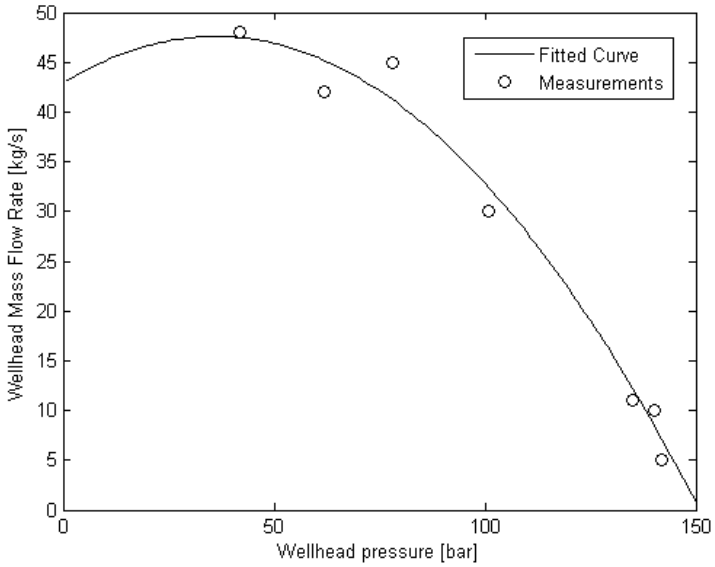


**Figure 8: Mass flow rate from IDDP-1 in a flow test carried out in the summer of 2011**

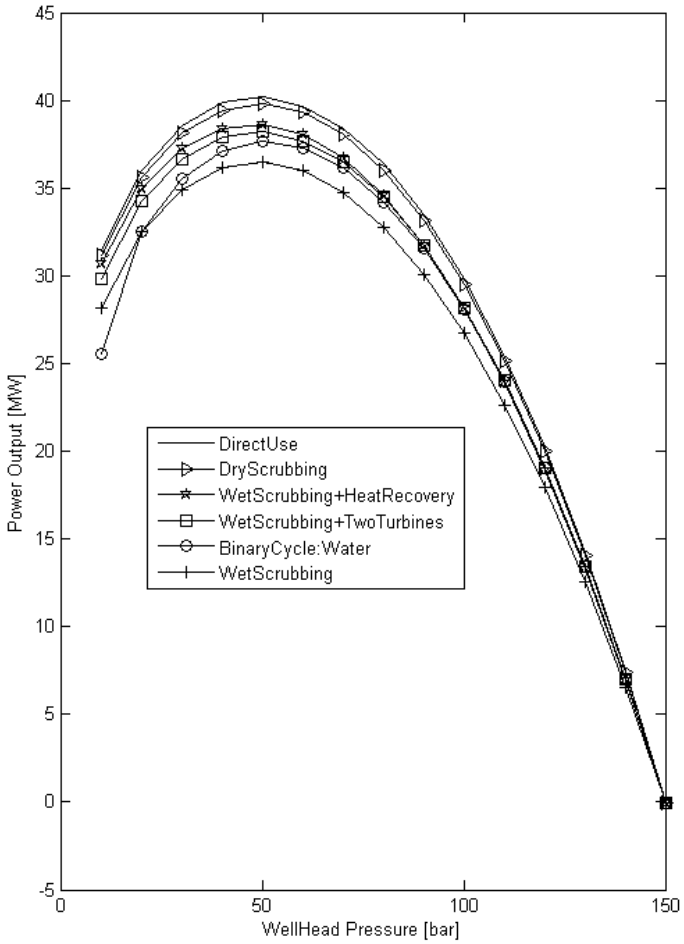


**Figure 9: Net Power Output of each corrosion mitigation method, using the mass flow rate from IDDP shown in figure 8**

undergone separation the steam enters the heat exchanger and gains superheat again. The following energy balance is used to calculate the enthalpy of the stream at state 5

$$\dot{m}_1(h_1 - h_2) = \dot{m}_4(h_5 - h_4) \quad (18)$$

Expansion of the superheated steam in the turbine is both dry and wet. In the end the fluid enters the condenser and cools down.

2.2.4 Single-Flash Cycle with Wet Scrubbing and an Additional Turbine

A process diagram is shown in figures 5. Before the superheated steam enters the traditional setup of wet scrubbing, it expands through a turbine without condensing. At the turbine outlet, the fluid has 20°C of superheat, which should be enough to ensure that no condensation takes place. The turbine expansion is similar to the one described above. The difference is that this is solely a dry expansion, and in order to keep a 20°C superheat at the outlet, the pressure at which the fluids properties would have crossed the saturated vapor curve is raised so that the temperature is 20°C higher and used as the turbine outlet pressure. After the steam has expanded through the turbine it undergoes wet scrubbing, enters the separator and expands through a turbine. At last the fluid is cooled down in a condenser.

2.2.5 Dry Steam Cycle with Dry Scrubbing

A process diagram is shown in figure 6. The superheated steam at state 1, enters a reaction vessel. The reaction vessel is a reference to any sort of equipment where chemicals are injected into the stream and react with or consume (absorption or adsorption) the HCl. The mixed flow is then passed through some sort of separator such as a bag house filter or electrostatic precipitator. The spent reactant is then recycled after being separated from the steam (Fisher et al. 1996).

Since it is hard to estimate the losses in this setup, it is assumed that they are similar to the ones in the laboratory bench tests that were conducted at Thermochem Laboratories in California, USA. The total heat loss for the processes ranged from 0−0.5%, in this case they will be assumed constant at 0.5%. Also, the total pressure drop was 0.14bar and will also be assumed constant. There was no measurable reduction in mass flow. (Hirtz et al. 2002)

After this, the geofluid expands through the turbine and is cooled down.

2.2.6 Binary Cycle with Condensation of Geofluid in Heat Exchanger

A process diagram is shown in figure 7. After the working fluid has received heat from the geofluid, it expands through a turbine. After that it is cooled down in a condenser and then pumped up to a higher pressure. Water is used as a working fluid. Models using ammonia, isobutene and isopentane as working fluids were also constructed but showed worse power outputs by a factor of 2, and will therefore be excluded from the study.

### 2.3 Execution of Computer Models

The computer models where executed using a geofluid with enthalpy at wellhead of 3100kJ/kg. A curve fitted to measurements from a flow test performed on IDDP-1 in the summer of 2011 was used for a wellhead mass flow rate in the models. The fitted curve along with the measured datapoints is shown in figure 8.

## 3 RESULTS

Figure 9 shows the net power output for all the mitigation methods. It is clear that the optimum wellhead pressure lies between 40-50bar. At these pressures, the power output of the mitigation methods differs by around 5MWe. It can be seen that wet scrubbing gives the smallest power output, while dry scrubbing gives the highest. This is not surprising as the superheat is lost in the wet scrubbing process. Wet scrubbing with heat recovery and wet scrubbing with an additional turbine are very similar; slightly better than the binary cycle.

Figure 10 shows the utilization efficiency for all the mitigation methods. Wet scrubbing has around 10% worse efficiency than dry scrubbing and wet scrubbing with an additional turbine. At higher pressures the dry scrubbing, wet scrubbing with an additional turbine, wet scrubbing with heat recovery and a binary cycle all have very similar utilization efficiency; with a difference of only around 4%.

It is interesting to see that although the mass flow rate at the wellhead decreases below 50bar, the condenser duty does not; see figure. 11. In order to decrease the condenser duty, the wellhead pressure has to be raised above 40bars, and from there it decreases with increasing wellhead pressure.

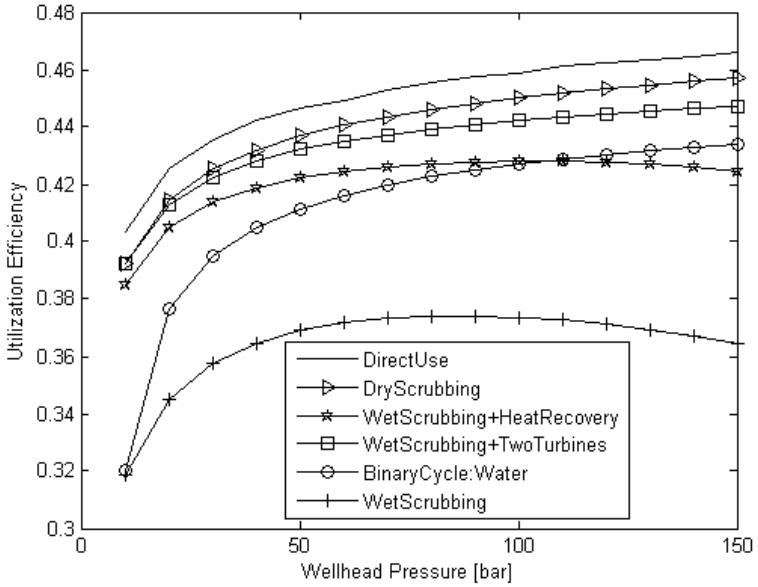


**Figure 10: Utilization efficiency of each corrosion mitigation method.**

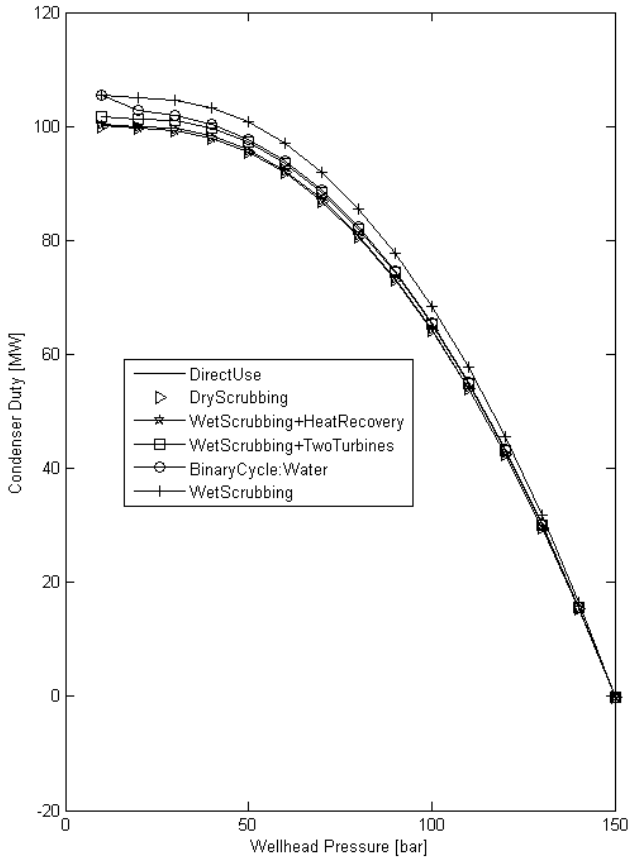


**Figure 11: Condenser duty of each corrosion mitigation method, using the mass flow rate from IDDP shown in figure 8.**

## 4 CONCLUSIONS

It is obvious that in terms of exergetic efficiency, dry scrubbing possesses great potential for improvement in corrosion mitigation. Having the best utilization efficiency, it will be a feasible choice when more development has taken place.

Expanding the steam in two turbines with intermediate wet scrubbing step as the steam exits the first turbine slightly above the saturation limit however appears to be a technically feasible approach that delivers almost the same efficiency. As this setup would not require much new technological development it may be immediately attractive

## 5 FURTHER WORK

The optimum wellhead pressure is not selected solely with the most power output of the borehole in mind. Many chemicals in the superheated geofluid may precipitate at a given pressure, causing erosion in the gathering equipment. Chemical analysis has to be performed in order to gain a better understanding on the behavior of the steam. This may affect the feasibility of individual corrosion mitigation.

## ACKNOWLEDGEMENTS

This work was funded by Geothermal Research Group (GEORG). It was also supported by Landsvirkjun and Mannvit hf.

## NOMENCLATURE

| | |
|---|---|
| $e$ | specific exergy (kJ/kg) |
| $\eta_p$ | pump efficiency |
| $\eta_{tw}$ | turbine efficiency working with wet steam |
| $\eta_{td}$ | turbine efficiency working with dry steam |
| $\eta_u$ | utilization efficiency |
| $h$ | enthalpy (kJ kg$^{-1}$) |
| $h_f$ | enthalpy of saturated liquid (kJ kg$^{-1}$) |
| $h_g$ | enthalpy of saturated vapor (kJ kg$^{-1}$) |
| $h_{gf}$ | enthalpy of geofluid (kJ kg$^{-1}$) |
| $h_{cm}$ | enthalpy of cooling medium (kJ kg$^{-1}$) |
| $\dot{m}$ | mass flow rate (kg s$^{-1}$) |
| $\dot{m}_{gf}$ | mass flow rate of geofluid (kg s$^{-1}$) |
| $\dot{m}_{cm}$ | mass flow rate of cooling medium (kg s$^{-1}$) |
| $\dot{m}_{wf}$ | mass flow rate of working fluid (kg s$^{-1}$) |
| $\dot{Q}$ | heat rate (kJ s$^{-1}$) |
| $T$ | temperature (°C) |
| $\dot{W}_t$ | turbine work rate (kJ s$^{-1}$) |
| $\dot{W}_p$ | pump work rate (kJ s$^{-1}$) |
| $x$ | quality of steam |

**REFERENCES**

Cengel, Yunus A., Boles, Michael A. 2006. Thermodynamics, An Engineering approach. McGraw-Hill, Singapore, 5th edition in SI units

DiPippo, R. 2008. Geothermal Power Plants: Principles, Applications, Case Studies and Environmental Impact. Butterworth-Heinemann. 2nd ed.

Fisher, D.W., Jung, D.B. 1996. Alternatives to Traditional Water Washing Used to Remove Impurities in superheated Geothermal Steam. *Geothermal Resources Council Transactions.,* Vol. 20, 737-741.

Hirtz, P., Miller, J., and Prabhu, E. 1990. Operational Results of a Drysteam Resource Chloride Corrosion Mitigation System. *Geothermal Resources Council Transactions,* Vol. 14, Part II, 1667-1675.

Hirtz, P., Buck, C., Kunzman, R. 1991. Current Techniques in Acid-Chloride Corrosion Control and Monitoring at The Geysers. *Proceedings,* Sixteenth Workshop on Geothermal Reservoir Engineering, Stanford University, Stanford, California, 83-95.

Hirtz, P. N., Broaddus, M. L., Gallup, D. L. 2002. Dry Steam Scrubbing for Impurity Removal from Superheated Geothermal Steam. *Geothermal Resources Council Transactions*, Vol. 26, 751-754.

Hjartarson, S., Saevarsdottir, G., Ingason, K., Palsson, B., Harvey, W., Utilization of Chloride Bearing High Enthalpy Geothermal Fluid. Geothermics Special Issue for the IDDP project 2013

Meeker, K. A., Haizlip, J. R. 1990. Factors Controlling pH and Optimum Corrosion Mitigation in Chloride-bearing Geothermal Steam at The Geysers. *Geothermal Resources Council Transactions,* Vol. 14, Part II, 1677-1684.

Viviani, E., Paglianti, A., Sabatelli, F., Tarquini, B. 1995. Abatement of Hydrogen Chloride in Geothermal Power Plants. World Geothermal Congress, 2421-2426.

Weres, O., Kendrick, C. 2010. Corrosion by HCl in Dry Steam Wells Controlled using Potassium Carbonate without Destoying Superheat. Geothermal Resources Council Transactions, Vol. 34, 1097-1104.